Research Article

Mitochonic acid 5 regulates mitofusin 2 to protect microglia

Jian Tan[#], Shuang-Xi Chen[#], Qing-Yun Lei, Shan-Qing Yi, Na Wu, Yi-Lin Wang, Zi-Jian Xiao[*], Heng Wu[*]

Graphical Abstract *Mitochonic acid-5 (MA-5) promotes the survival of microglial BV-2 cells under lipopolysaccharides (LPS)-induced inflammation via mitofusin 2 (Mfn2)-associated mitophagy*
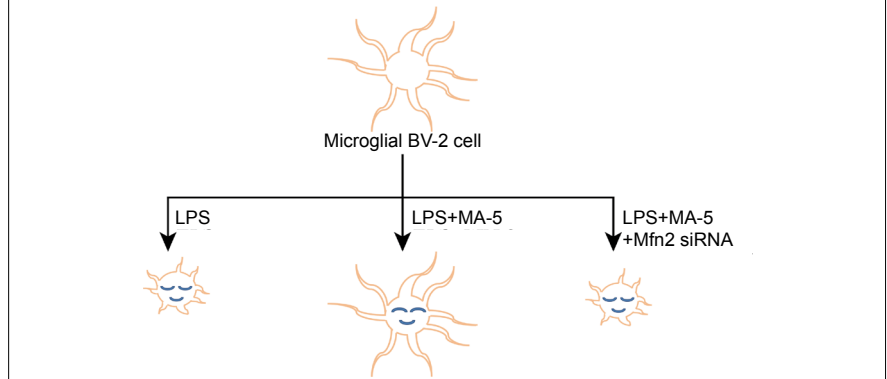
Abstract

Microglial apoptosis is associated with neuroinflammation and no effective strategies are currently available to protect microglia against inflammation-induced apoptosis. Mouse microglial BV-2 cells (5×10^6) were incubated with 10 μg/mL lipopolysaccharides for 12 hours to mimic an inflammatory environment. Then the cells were co-cultured with mitochonic acid 5 (MA-5) for another 12 hours. MA-5 improved the survival of lipopolysaccharide-exposed cells. MA-5 decreased the activity of caspase-3, which is associated with apoptosis. MA-5 reduced the number of terminal deoxynucleotidyl transferase-mediated dUTP-biotin nick end labeling-positive cells, and increased adenosine triphosphate levels in cells. MA-5 decreased the open state of the mitochondrial permeability transition pore and reduced calcium overload and diffusion of second mitochondria-derived activator of caspase (Smac). MA-5 decreased the expression of apoptosis-related proteins (mitochondrial Smac, cytoplasmic Smac, pro-caspase-3, cleaved-caspase-3, and caspase-9), and increased the levels of anti-apoptotic proteins (Bcl2 and X-linked inhibitor of apoptosis protein), mitochondria-related proteins (mitochondrial fusion protein 2, mitochondrial microtubule-associated proteins 1A/1B light chain 3B II), and autophagy-related proteins (Beclin1, p62 and autophagy related 5). However, MA-5 did not promote mitochondrial homeostasis or decrease microglial apoptosis when Mitofusin 2 expression was silenced. This shows that MA-5 increased Mitofusin 2-related mitophagy, reversed cellular energy production and maintained energy metabolism in BV-2 cells in response to lipopolysaccharide-induced inflammation. These findings indicate that MA-5 may promote the survival of microglial cells via Mitofusin 2-related mitophagy in response to lipopolysaccharide-induced inflammation.

Key Words: apoptosis; autophagy related 5; Beclin1; BV-2 cells; caspase-3; inflammation; lipopolysaccharide; mitophagy; Smac; survival

Chinese Library Classification No. R453; R741; R364.5

Introduction

Neuroinflammation is highly involved in various chronic diseases of the nervous system (Shen et al., 2017). However, there are currently no promising strategies available to prevent, or at least to slow, the progression of neuroinflammation. This inflammation, caused by calcium overload, mitochondrial damage, oxidative/nitrosative stress and disrupted energy production in neurons (Fuhrmann and Brüne, 2017; Griffiths et al., 2017) leads to synapse dysfunction, blood-brain barrier disruption, and neuronal death (Das et al., 2017; Calabrese et al., 2018). Lipopolysaccharides (LPS), large molecules present on the membranes of Gram-negative bacteria, regulates proinflammatory cytokines (Kitazawa et al., 2005), initiates a strong immune response in mammalian cells (Kim et al., 2019) and activates downstream inflammation-associated signaling pathways (Cochet and Peri, 2017; Yu et al., 2017). LPS is important as a prototypical microbe-derived activator of Toll-like receptor 4-dependent signaling, which subsequently stimulates activation of a cascade of pro- and anti-inflammatory mediators (Płóciennikowska et al., 2015) and nitric oxide (Abhimannue et al., 2016). LPS stimulates microglial cells by triggering multiple downstream signaling pathways, including the mitogen-activated protein

Department of Neurology, The First Affiliated Hospital of University of South China, Hengyang, Hunan Province, China
*Correspondence to: Heng Wu, PhD, 2915176817@qq.com; Zi-Jian Xiao, PhD, zijian6340@21cn.com.
https://orcid.org/0000-0002-6569-4651 (Heng Wu)
#Both authors contributed equally to this work.

kinase signaling cascade (Lampron et al., 2013) to induce neuroinflammatory cytokine production and degeneration of neurons *in vivo* (Dulla et al., 2016).

Microglia, first discovered using a platinum stain in 1899 (Walker et al., 2014), defend against injuries caused by chronic and acute stress in response to neurological damage (Kettenmann et al., 2011). Specific microglial functions can be neuroprotective (Ransohoff and Perry, 2009; Prinz and Priller, 2014; Fei et al., 2020). Activated microglia can promote regeneration of severed axons, secretion of neurotrophic factors, and the removal of potentially deleterious debris (Streit, 2002; Chen et al., 2012; Rice et al., 2015). Loss of microglia exacerbates brain injury (Szalay et al., 2016). Altered microglial function is associated with multiple human disorders, including stroke, Alzheimer's disease, depression, and Parkinson's disease, and with dysfunction in experimental animal models (Block et al., 2007; Denes et al., 2010; Faustino et al., 2011; Brown and Neher, 2014). Damaged microglia promote the release of proinflammatory factors to increase the inflammatory response (Chuang et al., 2017; Shen et al., 2017). As a consequence, protecting microglia against apoptosis may be a potential strategy for the treatment of neuroinflammation (Wang et al., 2017).

Attempts to target individual molecules that may reduce the pathological impact of neuroinflammation have been made. Such approaches have counteracted microglial apoptosis by inducing survival-proactive molecules. Mitochonic acid 5 (MA-5), an analogue of indole-3-acetic acid originally isolated from plants (Suzuki et al., 2016), improves mitochondrial function by reducing mitochondrial oxidative stress and accelerating mitochondrial energy metabolism (Matsuhashi et al., 2017). MA-5 upregulates cellular adenosine triphosphate (ATP) levels and protects fibroblasts from cell death in patients suffering from mitochondrial diseases (Suzuki et al., 2015). In addition, MA-5 can increase cardiovascular and kidney respiration in a mitochondrial disease mouse model (Nakada et al., 2001), resulting in prolonged survival (Suzuki et al., 2016). MA-5 has also been investigated in patients with mitochondrial disease, renal tubular injury, and cardiac myocyte damage (Suzuki et al., 2016).

Because of the interdependent mechanisms associated with neuroinflammation, we searched for other MA-5 targets that could ameliorate neuroinflammation. Mitochondria are dynamic organelles that undergo continuous fission and fusion (Mozdy et al., 2000). Mitochondrial dynamics are closely associated with apoptosis (Neuspiel et al., 2005); in particular, mitochondrial fission accelerates apoptosis (Xian and Liou, 2019). Mitophagy, a cellular response to mitochondrial damage, is associated with mitochondrial dynamics (Xiao et al., 2017; Zhou et al., 2017b). Mitofusin 2 (MFN2), a mitochondrial GTPase, has an essential role in mitochondrial dynamics, including in mitochondrial fusion regulation, transport, mitophagy, mitochondrial DNA stability, and mitochondria-endoplasmic reticulum interactions (Misko et al., 2010). A well-established role of MFN2 is regulation of mitochondrial fusion and mitophagy (Chandhok et al., 2018). In response to LPS-related inflammation injury, mitophagy activated by MFN2 helps injured mitochondria fuse with lysosomes to ensure mitophagy activation (Farmer et al., 2017; Vacek et al., 2018).

Given the protective roles of MA-5 toward mitochondria during neuroinflammation, we hypothesized that MA-5 may have a protective effect on the survival of BV-2 cells following LPS-induced neuroinflammation. The current study evaluated the effects of MA-5 on microglial apoptosis via MFN2-related mitophagy.

Materials and Methods

Cell culture and treatments

Mouse BV-2 cells purchased from the Cell Bank of Type Culture Collection of the Chinese Academy of Sciences were cultured in Dulbecco's Modified Eagle's medium (Cat# 11995065, Thermo Fisher Scientific, Waltham, MA, USA) supplemented with 10% inactivated fetal bovine serum (Cat# 10099141, Thermo Fisher Scientific) and 1% penicillin/streptomycin (Cat# P1400, Solarbio Science & Technology Co., Beijing, China) in 75-cm^2 cell culture plates (Cat# 430167, Corning, Corning, NY, USA) at 37°C in a humidified 5% CO_2 atmosphere.

To investigate the effect of MA-5 (Cat# 1354707-41-7, Selleck Chemicals, Houston, MO, USA) on inflammatory injury *in vitro*, mouse BV-2 cells (5 × 10^6 cells per well) were incubated with 10 μg/mL LPS (Cat# L8880, Solarbio Science & Technology Co.) for 12 hours to mimic an inflammatory environment (Van Nostrand et al., 2017). Cells were treated under three different conditions: i) co-cultured with MA-5 at various concentrations (0–10 μM) for 12 hours; ii) co-cultured with MA-5 at 5 μM; and iii) co-cultured with MA-5 at 5 μM following transfection with small interfering RNA (siRNA) against Mfn2 (a negative control of cells transfected with vehicle was also prepared).

Cell viability assessment

A 3-(4,5-dimethylthiazol-2-yl)-2,5-diphenyltetrazolium bromide (MTT) assay was performed as described with minor modifications (Lei et al., 2018; Chen et al., 2019, 2020). A terminal deoxynucleotidyl transferase-mediated dUTP-biotin nick end labeling (TUNEL) assay was performed using the one-step TUNEL kit (Cat# C1090, Beyotime Institute of Biotechnology, Shanghai, China) according to the manufacturer's instructions. After washing with phosphate buffer saline (PBS), the cells were fixed with 3.7% paraformaldehyde for 15 minutes. After washing the cells three times with PBS, the samples were incubated with proteinase K and the TUNEL reaction reagents in the dark for 2 hours at 37°C. After washing the cells with PBS a further three times, samples were stained with 4′,6-diamidino-2-phenylindole (Cat# P36935; Gibco, Thermo Fisher Scientific) and mounted.

Flow cytometric analysis of calcium

After rinsing with PBS, samples were incubated with Fluo-2 (a molecular probe; Cat# AAT-21116; AAT Bioquest, Sunnyvale, CA, USA) in the dark at 37°C for 30 minutes. Excess Fluo-2 was then removed by washing with PBS. After digestion with 0.25% pancreatin, centrifugation, and resuspension in PBS, flow cytometric analysis was performed (Sysmex Partec GmbH, Görlitz, Germany), with excitation at 506 nm and emission at 526 nm. For each group, 10,000 cells were used to calculate the calcium content, with analysis by Flowmax software (Sysmex Partec GmbH).

Detection of mitochondrial membrane potential and the rate of mPTP opening

Cells were gently washed with PBS, then incubated with 10 mg/mL MitoProbe JC-1 (Cat# C2006, Beyotime Institute of Biotechnology) in the dark for about 30 minutes at 37°C. A mitochondrial permeability transition pore (mPTP) opening assay was performed as described, using a well-established calcein cobalt loading procedure with a calcein-acetoxymethyl ester (Cat# HY-D0041; MedChemExpress, Monmouth Junction, NJ, USA) (Tallman et al., 2017). After three 5 minute washes in PBS, cells were incubated with a solution containing 2 μM calcein-acetoxymethyl ester and 8 μM cobalt chloride (Cat# H9060; Solarbio Science & Technology Co.) for more than 30 minutes in the dark.

Detection of ATP production

After washing with cold PBS, cells were lysed and then

processed using a luciferase-based ATP assay kit (Cat# S0026; Beyotime Institute of Biotechnology) according to the manufacturer's instructions. ATP production was detected using a microplate reader.

ROS and cardiolipin analysis
After three 5-minute washes in PBS, cells were incubated with the reactive oxygen species (ROS) probe, dihydroethidium (Molecular Probes; Cat# D1168; Thermo Fisher Scientific) or 10-N-nonyl acridine orange [a molecular probe; 2 mM; Cat# A1301; Thermo Fisher Scientific (binds to non-oxidized cardiolipin and generates the green fluorescence) (Hambright et al., 2017)] in the dark at 37°C for 30 minutes. To remove unattached probe, cells were washed with PBS.

Detection of caspase 3/9 activity
Caspase 3/9 activity was measured spectrophotometrically as described previously (Liu et al., 2017a). Caspase 3/9 activity was detected using a caspase 3/9 activity kit (Cat# K118-25; Beyotime Institute of Biotechnology) according to the manufacturer's protocol. DEVD-p-NA substrate or LEHD-p-NA substrate (5 μL at 4 mM) at a final concentration of 200 μM were added to samples at 37°C for 1 or 2 hours. A wavelength of 405 nM was used to detect caspase 3/9 activity.

Western blot analysis
Tissue preparation and western blotting were performed as described with minor modifications (Li et al., 2017; Xu et al., 2017). Cells were trypsinized, washed, incubated with RIPA buffer at 4°C for 30 minutes, followed by centrifugation at 10,000 × g at 4°C for 10 minutes. The collected supernatant was heated in loading buffer and separated by polyacrylamide gel electrophoresis. Proteins were then transferred to polyvinylidene fluoride membranes. After blocking with 5% non-fat milk (Cat# D8340; Solarbio Science & Technology Co.) for 1 hour at room temperature, membranes were incubated with the primary antibodies listed in **Table 1** diluted in 5% non-fat milk in Tris-buffered saline-Tween 20 overnight at 4°C. After washing three times with Tris-buffered saline-Tween 20, membranes were incubated with secondary antibodies: goat anti-rabbit IgG (H+L) + goat anti-mouse IgG (H+L), horseradish peroxidase conjugate (Cat# BA1056; 1:3000; Wuhan Boster Biological Technology, Wuhan, China) or donkey anti-goat IgG (H+L), horseradish peroxidase conjugate (Cat# ab6885; 1:2000; Abcam, Cambridge, UK) for 1.5 hours at room temperature. The immunoreactive bands were then visualized using an enhanced chemiluminescent liquid detection kit (Cat# 1705060; Bio-Rad, Hercules, CA, USA). Signal intensities were quantified using ImageJ 5.0 software (National Institutes of Health, Bethesda, MD, USA). Each immunoblot was normalized to the corresponding signal for β-actin or TOM20.

Immunofluorescence staining
Tissue preparation and immunofluorescence staining were performed as described with minor modifications (Chen et al., 2015b; Jiang et al., 2016). Samples were fixed in 3.7% paraformaldehyde, washed and incubated overnight at 4°C with rabbit anti-second mitochondria-derived activator of caspase (Smac) antibody (1:2000; Cat# ab8115; Abcam). Samples were then washed and incubated with Alexa Fluor® 594 fluorescence-labeled goat anti-mouse IgG (1:5000; Cat# A-21155; Invitrogen, Thermo Fisher Scientific) at room temperature for 1.5 hours. Samples were then washed, stained with 4′,6-diamidino-2-phenylindole (Cat# P36935; Gibco, Thermo Fisher Scientific), and mounted.

RNA interference
siRNAs against Mfn2 were produced by Shanghai GenePharma Co., China. The Mfn2 siRNA sequences were sense, 5′-CCT GCA GTU ATA CAU UGU CAT-3′ and anti-sense, 5′-CUA TCG ATG CAT ACA CAG GUT-3′. The control siRNA sequences were

Table 1 | Primary antibodies used for western blot analysis

Antibody	Source	Dilution	Catalogue	Company
Pro-caspase-3	Rabbit	1:1000	9662	Cell Signaling Technology
Cleaved-caspase-3	Rabbit	1:1000	9664	Cell Signaling Technology
Smac	Rabbit	1:1000	ab8115	Abcam
Bax	Rabbit	1:2000	5023	Cell Signaling Technology
Bcl2	Rabbit	1:1000	3498	Cell Signaling Technology
caspase 9	Rabbit	1:1000	ab32539	Abcam
Mito-LC3II	Rabbit	1:1000	3868	Cell Signaling Technology
p62	Mouse	1:1000	ab56416	Abcam
Beclin1	Rabbit	1:1000	3495	Cell Signaling Technology
Atg5	Rabbit	1:1000	12994	Cell Signaling Technology
Mfn2	Rabbit	1:1000	ab50838	Abcam
CIII-core2	Mouse	1:1000	459220	Invitrogen
CII-30	Mouse	1:1000	ab110410	Abcam
CIV-II	Mouse	1:1000	ab110268	Abcam
x-IAP	Goat	1:1000	ab205719	Abcam
TOM20	Mouse	1:1000	ab56783	Abcam
β-Actin	Mouse	1:1000	ab8226	Abcam

Atg5: Autophagy related 5; Mfn2: Mitofusin 2; mito-LC3II: mitochondrial microtubule-associated proteins 1A/1B light chain 3B II; Smac: second mitochondria-derived activator of caspase; x-IAP: X-linked inhibitor of apoptosis protein.

sense 5′-CTC CTC CAU GGU AGA UTC CAU-3′ and anti-sense, 5′-AUG GUC AUT UCG UUT CAG TGA-3′. After cells were washed in PBS, Lipofectamine® 2000 reagent (Solarbio Science & Technology Co.) was used for siRNA transfection (Shi et al., 2018). The transfection was performed for 72 hours and the transfection efficiency was confirmed by western blot analysis.

Image analysis
Two people who were blind to the treatment group performed image analysis. All images were captured using a laser confocal microscope (Cat# TCS SP5; Leica Microsystems GmbH, Wetzlar, Germany). To calculate the number of cells, at least five fields in a sample were randomly selected. The number of cells was counted using ImageJ 5.0 software. The mean from one series of stained sections was regarded as one sample.

Statistical analysis
Data from at least three independent experiments expressed as the mean ± standard error of mean (SEM) were analyzed by SigmaStat version 4.0 software (Systat Software, San Diego, CA, USA) via one-way analysis of variance, followed by Bonferroni's or Dunnett's *post hoc* test. $P < 0.05$ represents a statistically significant difference.

Results
MA-5 protects BV-2 cells against apoptosis induced by LPS
To investigate the protective effect of MA-5 on LPS-induced apoptosis of mouse BV-2 cells, MTT, caspase-3 activity, and TUNEL assays were performed. The MTT assay revealed that, in comparison with the vehicle control, the cell survival rate was significantly reduced in response to LPS treatment. Compared with the LPS-treated group, 5 and 10 μM MA-5 increased the cell survival rate of LPS-treated BV-2 cells (**Figure 1A**).

It was also observed that, in comparison with the vehicle control, caspase-3 activity, which is associated with apoptosis,

was increased after LPS treatment, whereas treatment of BV-2 cells with 5 and 10 μM MA-5 decreased caspase-3 activity (**Figure 1B**). The TUNEL assay revealed that after LPS treatment of BV-2 cells, the number of TUNEL-positive cells was increased but this number was decreased by 5 and 10 μM MA-5 in LPS-induced BV-2 cells (**Figure 1C** and **D**). These results revealed that 5 and 10 μM MA-5 reduced microglial BV-2 cell death induced by LPS. We therefore selected 5 μM, the minimum protective concentration of MA-5 [also observed in our previous study (Lei et al., 2018)] for subsequent experiments.

MA-5 reverses the mitochondrial damage induced by LPS
To further evaluate the protective role of MA-5 on LPS-induced apoptosis of BV-2 cells, mitochondrial membrane potential was measured. MitoProbe JC-1 staining demonstrated that, in comparison with the vehicle control, the ratio of red fluorescence intensity (an indicator of increased mitochondrial membrane potential)/green fluorescence intensity (an indicator of reduced mitochondrial membrane potential) was decreased in BV-2 cells following LPS treatment; however, in comparison with the LPS-treated group, MA-5 treatment rescued the LPS-induced reduction of the mitochondrial membrane potential (**Figure 2A** and **B**).

Following LPS treatment, the rate of mPTP opening (an early event causing mitochondrial protein leakage during mitochondrial apoptosis) was increased, whereas treatment with MA-5 decreased the mPTP opening rate compared with the LPS-treated group (**Figure 2C**). Cytoplasmic calcium levels analyzed by flow cytometry indicated that MA-5 treatment alleviated the LPS-induced cellular calcium overload (leading to apoptosis) (**Figure 2D**). Immunofluorescence staining for Smac demonstrated that Smac diffusion into the cytoplasm and/or nucleus was increased by LPS treatment but decreased by MA-5 treatment (**Figure 2E**). Western blot analysis showed that LPS treatment increased the levels of apoptosis-related proteins, including mitochondrial Smac, cytoplasmic Smac, pro-caspase-3, cleaved-caspase-3, caspase-9 and Bax, whereas treatment with MA-5 reduced the LPS-induced effect on mitochondrial Smac, cytoplasmic Smac, pro-caspase-3, cleaved-caspase-3 and caspase-9 expression in BV-2 cells. Additionally, LPS treatment decreased levels of anti-apoptotic proteins (Bcl-2 and X-linked inhibitor of apoptosis), whereas treatment with MA-5 increased Bcl-2, X-linked inhibitor of apoptosis levels in BV-2 cells compared with LPS-stimulated cells (**Figure 2F–L**).

MA-5 treatment increases MFN2-related mitophagy activity
To explore whether MA-5 can influence apoptosis via mitophagy, western blotting and immunofluorescence staining were performed. Western blot analysis indicated that, after LPS treatment of BV-2 cells, levels of MFN2, mitochondrial microtubule-associated proteins 1A/1B light chain 3B II, Beclin1, p62, and autophagy related 5 (indicative of mitophagy) were decreased; however, these above proteins levels were increased by MA-5 treatment. In MFN2 knockdown cells, treatment with MA-5 was unable to block the effects of LPS on these proteins (**Figure 3A–F**).

Caspase-9 activity was reduced in LPS-stimulated BV-2 cells, whereas treatment with MA-5 increased caspase-9 activity. However, following siRNA inhibition of Mfn2, treatment with MA-5 was unable to alter caspase-9 activity (**Figure 3G**).

MA-5-activated mitophagy reverses cellular energy production and maintains energy metabolism
Despite their role in apoptosis, mitochondria also control oxidative stress and energy metabolism to maintain normal cell functions (Zhou et al., 2017a). To explore whether MA-5 can influence cellular energy production under inflammation,

analysis of ATP levels, ROS and cardiolipin was performed. The level of ATP was decreased in LPS-stimulated BV-2 cells. MA-5 treatment reduced the effects of LPS, causing an increase in ATP levels. Furthermore, the effects of MA-5 were decreased following Mfn2 silencing (**Figure 4A**). Western blot analysis demonstrated LPS decreased the expression of several proteins that are part of the mitochondrial respiratory complexes (crucial for ATP generation), including CIII-core2, CII-30, and CIV-II; MA-5 inhibited the effects of LPS, causing the levels of these proteins to increase. Additionally, siRNA inhibition of Mfn2 reduced the effects of MA-5 on the protein levels of these proteins (**Figure 4B–E**).

ROS levels, an indicator of oxidative stress (Sarna et al., 2016), were substantially increased in BV-2 cells by LPS, and this effect was reduced by treatment with MA-5. Silencing Mfn2 inhibited the effect of MA-5 on ROS levels (**Figure 4F** and **G**). A similar pattern was observed for levels of cardiolipin (**Figure 4H**) (Kawalec et al., 2015).

Discussion

Previous studies, including ours, have indicated that MA-5 attenuates tumor necrosis factor-α-mediated neuronal inflammation by activating Parkin-related mitophagy, augmenting the adenosine monophosphate-activated protein kinase-Sirt3 pathways (Huang et al., 2019), and increasing Bnip3-related mitophagy (Lei et al., 2018). Promotion of survival is essential for ameliorating nervous system disorders (Chen et al., 2015a; Zhang et al., 2019) and the findings of the present study demonstrate the protective effects of MA-5 on BV-2 cells under LPS-induced inflammation.

Currently, microglial inflammatory responses are not considered to be inevitably neurotoxic. Previous studies have shown that exogenous microglia protect against various forms of ischemic brain injury (Kitamura et al., 2004, 2005). Additionally, microglia can be beneficial in Alzheimer's disease (El Khoury et al., 2007) and stroke (Lalancette-Hébert et al., 2007). Promotion of microglial functions may be crucial for neuronal survival under pathological conditions (Vinet et al., 2012). Apoptosis of microglia hinders recovery following damage caused by chronic neuroinflammation in the nervous system (Ölmestig et al., 2017). In the current study, we observed that MA-5 reduced the LPS-induced apoptosis of BV-2 cells.

Calcium overload, oxidative stress and inflammatory cytokines can induce apoptosis in microglia (Shen et al., 2017). Microglial apoptosis is primarily caused by mitochondrial damage (Wang et al., 2017; Zhou et al., 2017a), which involves reduced mitochondrial membrane potential, mPTP opening and mitochondrial calcium overload (Zhou et al., 2017b). Inflammation also induces mitochondrial fission (Liu et al., 2017b) and excessive mitochondrial fission leads to uneven mitochondrial DNA distribution into daughter mitochondria, resulting in insufficient ATP production (Ju et al., 2017). Accumulating evidence demonstrates that MA-5 can protect mitochondria (Suzuki et al., 2016; Matsuhashi et al., 2017). The findings of the present study indicated that MA-5 promotes mitochondrial functions under inflammation conditions.

Mitophagy can block mitochondrial apoptotic signaling (Yan et al., 2018), and is activated to degrade damaged mitochondria (Xiao et al., 2017). Mitophagy maintains the quality, quantity, and homeostasis of mitochondria (Jin et al., 2018) to promote mitochondrial function and suppress the mitochondrial apoptosis pathway (Onphachanh et al., 2017; Zhou et al., 2017c). In response to activated mitophagy, the ROS generated by mitochondria are reduced, cellular calcium overload is decreased through reduced leakage of mitochondrial calcium, and apoptosis mediated by mitochondria is suppressed
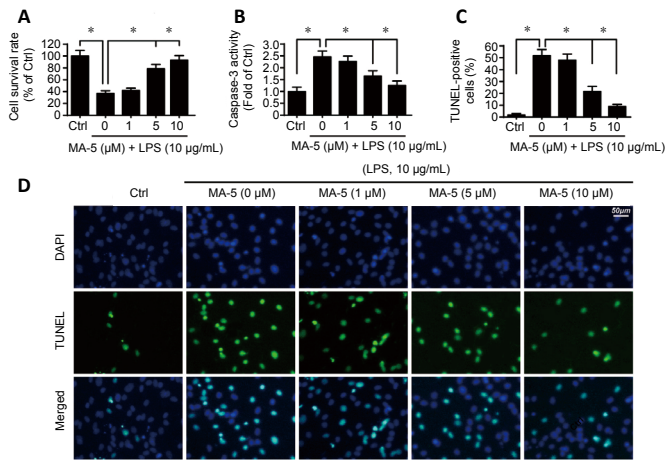
Figure 1 | **MA-5 reduces LPS-induced apoptosis of BV-2 cells in a dose-dependent manner.**
(A) MTT assays to detect cell survival. (B) Caspase-3 activity. (C) TUNEL assays to investigate cell numbers. Data are expressed as the mean ± SEM (n = 3). *P < 0.05 (one-way analysis of variance with Bonferroni's *post hoc* test). (D) TUNEL assays of BV-2 cells. After LPS treatment of BV-2 cells, the number of TUNEL-positive cells was increased, but was decreased by MA-5 treatment of LPS-induced BV-2 cells. Ctrl: Vehicle control group; DAPI: 4′,6-diamidino-2-phenylindole; LPS: lipopolysaccharides; MA-5: mitochonic acid 5; MTT: 3-(4,5-dimethylthiazol-2-yl)-2,5-diphenyltetrazolium bromide; TUNEL: terminal deoxynucleotidyl transferase-mediated dUTP-biotin nick end labeling.
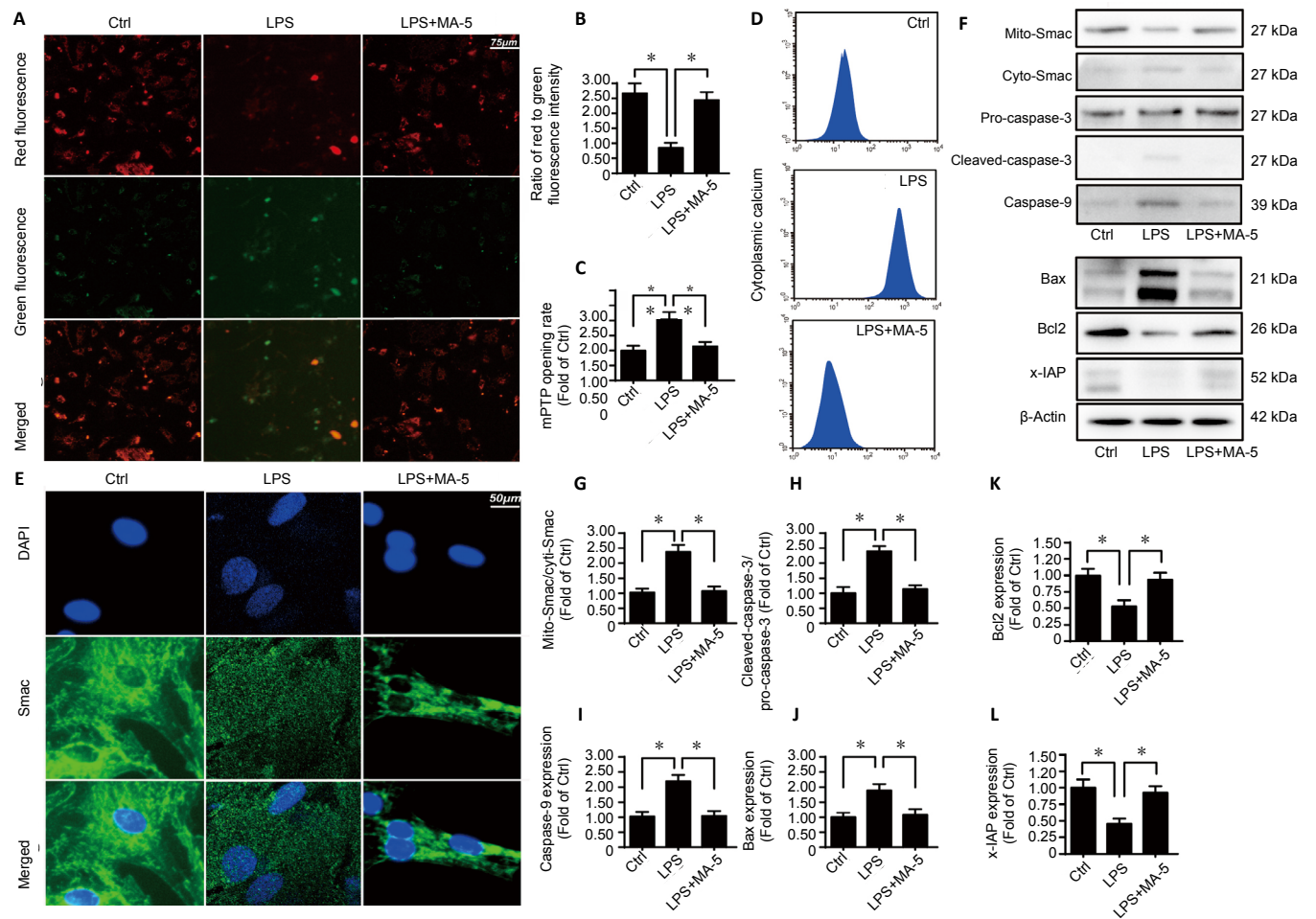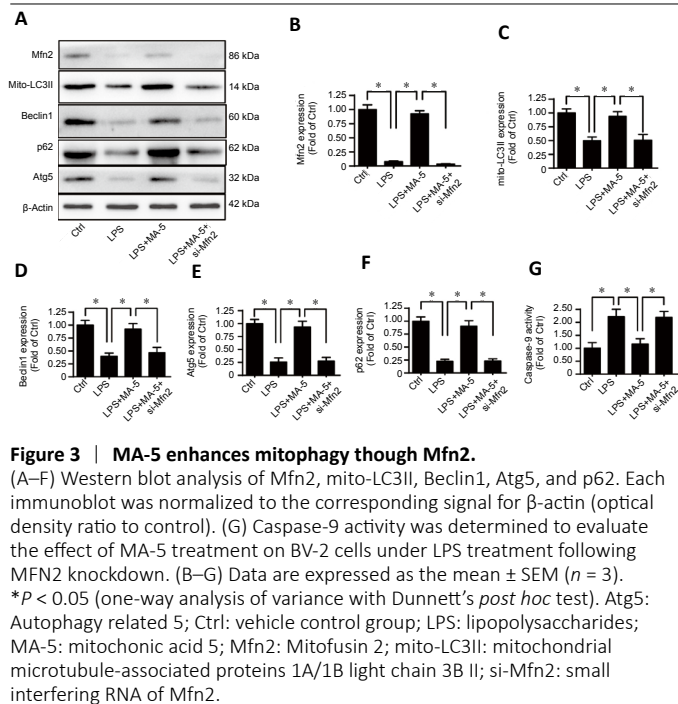

Figure 2 | **MA-5 protects the function of mitochondria.**
(A, B) Mitochondrial membrane potential. Red fluorescence: an indicator of increased mitochondrial membrane potential; green fluorescence: an indicator of reduced mitochondrial membrane potential. Compared with vehicle control, the ratio of red/green fluorescence intensity was decreased; and MA-5 inhibited this effect. (C) mPTP opening rate. (D) Cellular calcium was detected using flow cytometry. (E) Immunofluorescence staining of Smac (green, Alexa Fluor® 594). Smac diffusion into the cytoplasm and/or nucleus was increased by LPS treatment but decreased by MA-5 treatment. (F—L) Western blot analysis of mito-Smac, cyto-Smac, pro-caspase-3, cleaved-caspase-3, caspase-9, Bax, Bcl2, and x-IAP. Each immunoblot was normalized to the corresponding signal for β-actin (optical density ratio to control). (B, C, G—L) Data are expressed as the mean ± SEM (n = 3). *P < 0.05 (one-way analysis of variance with Dunnett's *post hoc* test). Ctrl: Vehicle control group; cyto-Smac: cytoplasmic second mitochondria-derived activator of caspase; DAPI: 4′,6-diamidino-2-phenylindole; LPS: lipopolysaccharides; MA-5: mitochonic acid 5; mito-Smac: mitochondrial second mitochondria-derived activator of caspase; mPTP: mitochondrial permeability transition pore; x-IAP: X-linked inhibitor of apoptosis protein.

through reduced release of pro-apoptotic factors from the mitochondria (Onphachanh et al., 2017). The formation of phagophores, autophagosomes and autophagolysosomes is regulated by autophagy-related proteins (Atgs). Atg1 and Beclin 1 participate in the early stages of autophagy and associations between autophagy related 5 and lipidation of Atg8 induce the formation of autophagosomes (Aparicio et al., 2016). LC3II is considered to be an autophagosomal marker (Tanida et al., 2004). Injured mitochondria are labeled with LC3II, which accelerates the degradation of defective

Figure 3 | MA-5 enhances mitophagy though Mfn2.
(A–F) Western blot analysis of Mfn2, mito-LC3II, Beclin1, Atg5, and p62. Each immunoblot was normalized to the corresponding signal for β-actin (optical density ratio to control). (G) Caspase-9 activity was determined to evaluate the effect of MA-5 treatment on BV-2 cells under LPS treatment following MFN2 knockdown. (B–G) Data are expressed as the mean ± SEM ($n = 3$). *$P < 0.05$ (one-way analysis of variance with Dunnett's *post hoc* test). Atg5: Autophagy related 5; Ctrl: vehicle control group; LPS: lipopolysaccharides; MA-5: mitochonic acid 5; Mfn2: Mitofusin 2; mito-LC3II: mitochondrial microtubule-associated proteins 1A/1B light chain 3B II; si-Mfn2: small interfering RNA of Mfn2.

mitochondria (Du et al., 2016; Quijano et al., 2016). p62 localizes to autophagosomes via interaction with LC3II and accumulates in response to autophagy (Bjørkøy et al., 2009). The present study demonstrates that MA-5 enhances mitophagy via MFN2.

Cardiolipin is oxidized following excessive oxidative stress, contributing to reduced activity of mitochondrial respiratory complexes (Hu et al., 2017; Zhou et al., 2017a). Despite their role in apoptosis, mitochondria also control oxidative stress and energy metabolism to maintain normal cellular functions (Zhou et al., 2017c). In somatic cells, an increase in ROS production, loss of cellular homeostasis, and reduced mitochondrial membrane potential and ATP content occur in response to impaired clearance of mitochondria (Chistiakov et al., 2014). MA-5 can affect the production of mitochondrial energy, the increase of mitochondrial respiration, and the scavenging of ROS (Boyko et al., 2017). The present study demonstrated that MA-5 alters energy production and oxidative stress in mitochondria.

While the results of the present study are promising, there are several limitations. We concentrated on the effect of MA-5 on the survival of BV-2 cells. Whether MA-5 can influence the migration and other biological processes of BV-2 cells need to be investigated. Additionally, experiments using animal disease models to test the effects of MA-5 are necessary.

Our study supports the beneficial functions of MA-5 on the survival of BV-2 cells, laying the foundation for indole-3-acetic acid analogues to ameliorate the consequences of neuroinflammation in a clinical setting. We hypothesize that MA-5 may be useful to promote microglial activity. Our observations lay the foundation for developing a novel approach to treat neurological disorders associated with microglial apoptosis.
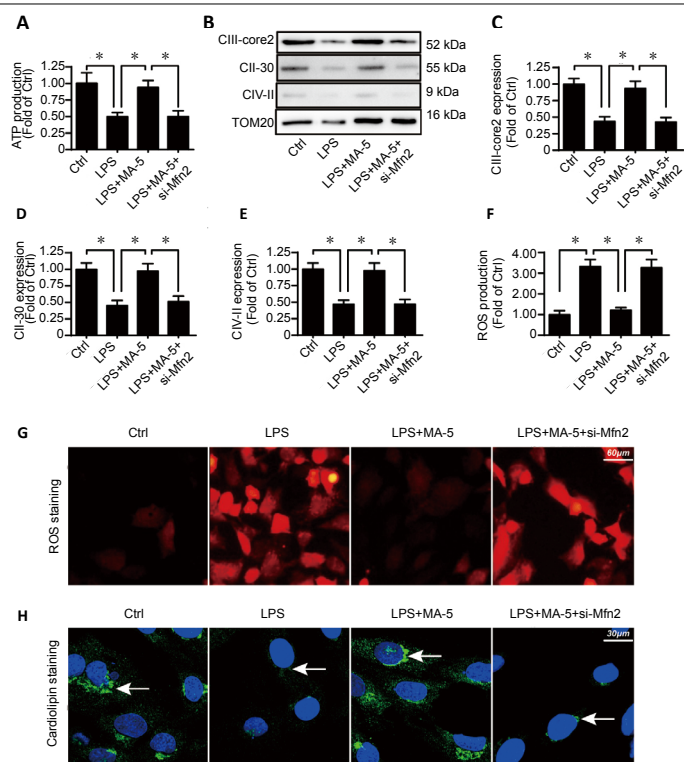
Figure 4 | MA-5 reduces oxidative stress and energy production in mitochondria of microglial BV-2 cells.
(A) ATP production. (B–E) Western blot analysis of CIII-core2, CII-30, and CIV-II. Each immunoblot was normalized to TOM20 of the control group). (F–G) ROS levels were detected using a ROS probe. (H) Cardiolipin level (arrows). (A, C–F) Data are expressed as the mean ± SEM ($n = 3$). *$P < 0.05$ (one-way analysis of variance with Dunnett's *post hoc* test). ATP: adenosine triphosphate; Ctrl: vehicle control group; LPS: lipopolysaccharides; MA-5: mitochonic acid 5; ROS: reactive oxygen species; si-Mfn2: small interfering RNA of Mfn2.

References

Abhimannue AP, Mohan MC, B PK (2016) Inhibition of tumor necrosis factor-α and interleukin-1β production in lipopolysaccharide-stimulated monocytes by methanolic extract of elephantopus scaber linn and identification of bioactive components. Appl Biochem Biotechnol 179:427-443.

Aparicio IM, Espino J, Bejarano I, Gallardo-Soler A, Campo ML, Salido GM, Pariente JA, Peña FJ, Tapia JA (2016) Autophagy-related proteins are functionally active in human spermatozoa and may be involved in the regulation of cell survival and motility. Sci Rep 6:33647.

Bjørkøy G, Lamark T, Pankiv S, Øvervatn A, Brech A, Johansen T (2009) Monitoring autophagic degradation of p62/SQSTM1. Methods Enzymol 452:181-197.

Block ML, Zecca L, Hong JS (2007) Microglia-mediated neurotoxicity: uncovering the molecular mechanisms. Nat Rev Neurosci 8:57-69.

Boyko AA, Troyanova NI, Kovalenko EI, Sapozhnikov AM (2017) Similarity and differences in inflammation-related characteristics of the peripheral immune system of patients with Parkinson's and Alzheimer's diseases. Int J Mol Sci 18:2633.

Brown GC, Neher JJ (2014) Microglial phagocytosis of live neurons. Nat Rev Neurosci 15:209-216.

Calabrese V, Santoro A, Monti D, Crupi R, Di Paola R, Latteri S, Cuzzocrea S, Zappia M, Giordano J, Calabrese EJ, Franceschi C (2018) Aging and Parkinson's disease: inflammaging, neuroinflammation and biological remodeling as key factors in pathogenesis. Free Radical Biol Med 115:80-91.

Chandhok G, Lazarou M, Neumann B (2018) Structure, function, and regulation of mitofusin-2 in health and disease. Biol Rev Camb Philos Soc 93:933-949.

Chen SL, Chen ZG, Dai HL, Ding JX, Guo JS, Han N, Jiang BG, Jiang HJ, Li J, Li SP, Li WJ, Liu J, Ma JX, Peng J, Sun GW, Shen YD, Tang PF, Liu Y, Wang GH, Wang XH, et al. (2015a) Repair, protection and regeneration of peripheral nerve injury. Neural Regen Res 10:1777-1798.

Chen SX, Hu CL, Liao YH, Zhao WJ (2015b) L1 modulates PKD1 phosphorylation in cerebellar granule neurons. Neurosci Lett 584:331-336.

Chen SX, He JH, Mi YJ, Shen HF, Schachner M, Zhao WJ (2020) A mimetic peptide of α2,6-sialyllactose promotes neuritogenesis. Neural Regen Res 15:1058-1065.

Chen S, Hou Y, Zhao Z, Luo Y, Lv S, Wang Q, Li J, He L, Zhou L, Wu W (2019) Neuregulin-1 accelerates functional motor recovery by improving motoneuron survival after brachial plexus root avulsion in mice. Neuroscience 404:510-518.

Chen Z, Jalabi W, Shpargel KB, Farabaugh KT, Dutta R, Yin X, Kidd GJ, Bergmann CC, Stohlman SA, Trapp BD (2012) Lipopolysaccharide-induced microglial activation and neuroprotection against experimental brain injury is independent of hematogenous TLR4. J Neurosci 32:11706-11715.

Chistiakov DA, Sobenin IA, Revin VV, Orekhov AN, Bobryshev YV (2014) Mitochondrial aging and age-related dysfunction of mitochondria. Biomed Res Int 2014:238463.

Chuang KA, Li MH, Lin NH, Chang CH, Lu IH, Pan IH, Takahashi T, Perng MD, Wen SF (2017) Rhinacanthin C alleviates amyloid-β fibrils' toxicity on neurons and attenuates neuroinflammation triggered by LPS, amyloid-β, and interferon-γ in glial cells. Oxid Med Cell Longev 2017:5414297.

Cochet F, Peri F (2017) The role of carbohydrates in the lipopolysaccharide (LPS)/Toll-like receptor 4 (TLR4) signalling. Int J Mol Sci 18:2318.

Das N, Mandala A, Naaz S, Giri S, Jain M, Bandyopadhyay D, Reiter RJ, Roy SS (2017) Melatonin protects against lipid-induced mitochondrial dysfunction in hepatocytes and inhibits stellate cell activation during hepatic fibrosis in mice. J Pineal Res 62:e12404.

Denes A, Thornton P, Rothwell NJ, Allan SM (2010) Inflammation and brain injury: acute cerebral ischaemia, peripheral and central inflammation. Brain Behav Immun 24:708-723.

Du K, Ramachandran A, Jaeschke H (2016) Oxidative stress during acetaminophen hepatotoxicity: Sources, pathophysiological role and therapeutic potential. Redox Biol 10:148-156.

Dulla YAT, Kurauchi Y, Hisatsune A, Seki T, Shudo K, Katsuki H (2016) Regulatory mechanisms of vitamin D(3) on production of nitric oxide and pro-inflammatory cytokines in microglial BV-2 cells. Neurochem Res 41:2848-2858.

El Khoury J, Toft M, Hickman SE, Means TK, Terada K, Geula C, Luster AD (2007) Ccr2 deficiency impairs microglial accumulation and accelerates progression of Alzheimer-like disease. Nat Med 13:432-438.

Farmer T, Reinecke JB, Xie S, Bahl K, Naslavsky N, Caplan S (2017) Control of mitochondrial homeostasis by endocytic regulatory proteins. J Cell Sci 130:2359-2370.

Faustino JV, Wang X, Johnson CE, Klibanov A, Derugin N, Wendland MF, Vexler ZS (2011) Microglial cells contribute to endogenous brain defenses after acute neonatal focal stroke. J Neurosci 31:12992-13001.

Fei F, Su N, Li X, Fei Z (2020) Neuroprotection mediated by natural products and their chemical derivatives. Neural Regen Res 15:2008-2015.

Fuhrmann DC, Brüne B (2017) Mitochondrial composition and function under the control of hypoxia. Redox Biol 12:208-215.

Griffiths HR, Gao D, Pararasa C (2017) Redox regulation in metabolic programming and inflammation. Redox Biol 12:50-57.

Hambright WS, Fonseca RS, Chen L, Na R, Ran Q (2017) Ablation of ferroptosis regulator glutathione peroxidase 4 in forebrain neurons promotes cognitive impairment and neurodegeneration. Redox Biol 12:8-17.

Hu SY, Zhang Y, Zhu PJ, Zhou H, Chen YD (2017) Liraglutide directly protects cardiomyocytes against reperfusion injury possibly via modulation of intracellular calcium homeostasis. J Geriatr Cardiol 14:57-66.

Huang D, Liu M, Jiang Y (2019) Mitochonic acid-5 attenuates TNF-α-mediated neuronal inflammation via activating Parkin-related mitophagy and augmenting the AMPK-Sirt3 pathways. J Cell Physiol 234:22172-22182.

Jiang Q, Chen S, Hu C, Huang P, Shen H, Zhao W (2016) Neuregulin-1 (Nrg1) signaling has a preventive role and is altered in the frontal cortex under the pathological conditions of Alzheimer's disease. Mol Med Rep 14:2614-2624.

Jin Q, Li R, Hu N, Xin T, Zhu P, Hu S, Ma S, Zhu H, Ren J, Zhou H (2018) DUSP1 alleviates cardiac ischemia/reperfusion injury by suppressing the Mff-required mitochondrial fission and Bnip3-related mitophagy via the JNK pathways. Redox Biol 14:576-587.

Ju C, Gao J, Hou L, Wang L, Zhang F, Sun F, Zhang T, Xu P, Shi Z, Hu F, Zhang C (2017) Neuroprotective effect of chondroitin sulfate on SH-SY5Y cells overexpressing wild-type or A53T mutant α-synuclein. Mol Med Rep 16:8721-8728.

Kawalec M, Boratyńska-Jasińska A, Beręsewicz M, Dymkowska D, Zabłocki K, Zabłocka B (2015) Mitofusin 2 deficiency affects energy metabolism and mitochondrial biogenesis in MEF cells. PLoS One 10:e0134162.

Kettenmann H, Hanisch UK, Noda M, Verkhratsky A (2011) Physiology of microglia. Physiol Rev 91:461-553.

Kim ME, Na JY, Park YD, Lee JS (2019) Anti-neuroinflammatory effects of vanillin through the regulation of inflammatory factors and NF-κB signaling in LPS-stimulated microglia. Appl Biochem Biotechnol 187:884-893.

Kitamura Y, Takata K, Inden M, Tsuchiya D, Yanagisawa D, Nakata J, Taniguchi T (2004) Intracerebroventricular injection of microglia protects against focal brain ischemia. J Pharmacol Sci 94:203-206.

Kitamura Y, Yanagisawa D, Inden M, Takata K, Tsuchiya D, Kawasaki T, Taniguchi T, Shimohama S (2005) Recovery of focal brain ischemia-induced behavioral dysfunction by intracerebroventricular injection of microglia. J Pharmacol Sci 97:289-293.

Kitazawa M, Oddo S, Yamasaki TR, Green KN, LaFerla FM (2005) Lipopolysaccharide-induced inflammation exacerbates tau pathology by a cyclin-dependent kinase 5-mediated pathway in a transgenic model of Alzheimer's disease. J Neurosci 25:8843-8853.

Lalancette-Hébert M, Gowing G, Simard A, Weng YC, Kriz J (2007) Selective ablation of proliferating microglial cells exacerbates ischemic injury in the brain. J Neurosci 27:2596-2605.

Lampron A, Elali A, Rivest S (2013) Innate immunity in the CNS: redefining the relationship between the CNS and Its environment. Neuron 78:214-232.

Lei Q, Tan J, Yi S, Wu N, Wang Y, Wu H (2018) Mitochonic acid 5 activates the MAPK-ERK-yap signaling pathways to protect mouse microglial BV-2 cells against TNFα-induced apoptosis via increased Bnip3-related mitophagy. Cell Mol Biol Lett 23:14.

Li J, Chen S, Zhao Z, Luo Y, Hou Y, Li H, He L, Zhou L, Wu W (2017) Effect of VEGF on inflammatory regulation, neural survival, and functional improvement in rats following a complete spinal cord transection. Front Cell Neurosci 11:381.

Liu L, Li H, Cui Y, Li R, Meng F, Ye Z, Zhang X (2017a) Calcium channel opening rather than the release of ATP causes the apoptosis of osteoblasts induced by overloaded mechanical stimulation. Cell Physiol Biochem 42:441-454.

Research Article

Liu Y, Liu K, Wang N, Zhang H (2017b) N-acetylcysteine induces apoptosis via the mitochondria-dependent pathway but not via endoplasmic reticulum stress in H9c2 cells. Mol Med Rep 16:6626-6633.

Matsuhashi T, Sato T, Kanno SI, Suzuki T, Matsuo A, Oba Y, Kikusato M, Ogasawara E, Kudo T, Suzuki K, Ohara O, Shimbo H, Nanto F, Yamaguchi H, Saigusa D, Mukaiyama Y, Watabe A, Kikuchi K, Shima H, Mishima E, et al. (2017) Mitochonic acid 5 (MA-5) facilitates ATP synthase oligomerization and cell survival in various mitochondrial diseases. EBioMedicine 20:27-38.

Misko A, Jiang S, Wegorzewska I, Milbrandt J, Baloh RH (2010) Mitofusin 2 is necessary for transport of axonal mitochondria and interacts with the Miro/Milton complex. J Neurosci 30:4232-4240.

Mozdy AD, McCaffery JM, Shaw JM (2000) Dnm1p GTPase-mediated mitochondrial fission is a multi-step process requiring the novel integral membrane component Fis1p. J Cell Biol 151:367-380.

Nakada K, Inoue K, Ono T, Isobe K, Ogura A, Goto YI, Nonaka I, Hayashi JI (2001) Inter-mitochondrial complementation: Mitochondria-specific system preventing mice from expression of disease phenotypes by mutant mtDNA. Nat Med 7:934-940.

Neuspiel M, Zunino R, Gangaraju S, Rippstein P, McBride H (2005) Activated mitofusin 2 signals mitochondrial fusion, interferes with Bax activation, and reduces susceptibility to radical induced depolarization. J Biol Chem 280:25060-25070.

Ölmestig JNE, Marlet IR, Hainsworth AH, Kruuse C (2017) Phosphodiesterase 5 inhibition as a therapeutic target for ischemic stroke: A systematic review of preclinical studies. Cell Signal 38:39-48.

Onphachanh X, Lee HJ, Lim JR, Jung YH, Kim JS, Chae CW, Lee SJ, Gabr AA, Han HJ (2017) Enhancement of high glucose-induced PINK1 expression by melatonin stimulates neuronal cell survival: Involvement of MT(2) /Akt/NF-κB pathway. J Pineal Res 63:e12427.

Płóciennikowska A, Hromada-Judycka A, Borzęcka K, Kwiatkowska K (2015) Co-operation of TLR4 and raft proteins in LPS-induced pro-inflammatory signaling. Cell Mol Life Sci 72:557-581.

Prinz M, Priller J (2014) Microglia and brain macrophages in the molecular age: from origin to neuropsychiatric disease. Nat Rev Neurosci 15:300-312.

Quijano C, Trujillo M, Castro L, Trostchansky A (2016) Interplay between oxidant species and energy metabolism. Redox Biol 8:28-42.

Ransohoff RM, Perry VH (2009) Microglial physiology: unique stimuli, specialized responses. Annu Rev Immunol 27:119-145.

Rice RA, Spangenberg EE, Yamate-Morgan H, Lee RJ, Arora RPS, Hernandez MX, Tenner AJ, West BL, Green KN (2015) Elimination of microglia improves functional outcomes following extensive neuronal loss in the hippocampus. J Neurosci 35:9977-9989.

Sarna LK, Sid V, Wang P, Siow YL, House JD, O K (2016) Tyrosol attenuates high fat diet-induced hepatic oxidative stress: potential involvement of cystathionine β-synthase and cystathionine γ-lyase. Lipids 51:583-590.

Shen Y, Guo X, Han C, Wan F, Ma K, Guo S, Wang L, Xia Y, Liu L, Lin Z, Huang J, Xiong N, Wang T (2017) The implication of neuronimmunoendocrine (NIE) modulatory network in the pathophysiologic process of Parkinson's disease. Cell Mol Life Sci 74:3741-3768.

Shi C, Cai Y, Li Y, Li Y, Hu N, Ma S, Hu S, Zhu P, Wang W, Zhou H (2018) Yap promotes hepatocellular carcinoma metastasis and mobilization via governing cofilin/F-actin/lamellipodium axis by regulation of JNK/Bnip3/SERCA/CaMKII pathways. Redox Biol 14:59-71.

Streit WJ (2002) Microglia as neuroprotective, immunocompetent cells of the CNS. Glia 40:133-139.

Suzuki T, Yamaguchi H, Kikusato M, Matsuhashi T, Matsuo A, Sato T, Oba Y, Watanabe S, Minaki D, Saigusa D, Shimbo H, Mori N, Mishima E, Shima H, Akiyama Y, Takeuchi Y, Yuri A, Kikuchi K, Toyohara T, Suzuki C, et al. (2015) Mitochonic acid 5 (MA-5), a derivative of the plant hormone indole-3-acetic acid, improves survival of fibroblasts from patients with mitochondrial diseases. Tohoku J Exp Med 236:225-232.

Suzuki T, Yamaguchi H, Kikusato M, Hashizume O, Nagatoishi S, Matsuo A, Sato T, Kudo T, Matsuhashi T, Murayama K, Ohba Y, Watanabe S, Kanno S-I, Minaki D, Saigusa D, Shinbo H, Mori N, Yuri A, Yokoro M, Mishima E, et al. (2016) Mitochonic acid 5 binds mitochondria and ameliorates renal tubular and cardiac myocyte damage. J Am Soc Nephrol 27:1925-1932.

Szalay G, Martinecz B, Lénárt N, Környei Z, Orsolits B, Judák L, Császár E, Fekete R, West BL, Katona G, Rózsa B, Dénes Á (2016) Microglia protect against brain injury and their selective elimination dysregulates neuronal network activity after stroke. Nat Commun 7:11499.

Tallman KA, Kim HYH, Korade Z, Genaro-Mattos TC, Wages PA, Liu W, Porter NA (2017) Probes for protein adduction in cholesterol biosynthesis disorders: Alkynyl lanosterol as a viable sterol precursor. Redox Biol 12:182-190.

Tanida I, Ueno T, Kominami E (2004) LC3 conjugation system in mammalian autophagy. Int J Biochem Cell Biol 36:2503-2518.

Vacek JC, Behera J, George AK, Kamat PK, Kalani A, Tyagi N (2018) Tetrahydrocurcumin ameliorates homocysteine-mediated mitochondrial remodeling in brain endothelial cells. J Cell Physiol 233:3080-3092.

Van Nostrand JL, Bowen ME, Vogel H, Barna M, Attardi LD (2017) The p53 family members have distinct roles during mammalian embryonic development. Cell Death Differ 24:575-579.

Vinet J, Weering HR, Heinrich A, Kälin RE, Wegner A, Brouwer N, Heppner FL, Rooijen Nv, Boddeke HWGM, Biber K (2012) Neuroprotective function for ramified microglia in hippocampal excitotoxicity. J Neuroinflammation 9:27.

Walker FR, Beynon SB, Jones KA, Zhao Z, Kongsui R, Cairns M, Nilsson M (2014) Dynamic structural remodelling of microglia in health and disease: a review of the models, the signals and the mechanisms. Brain Behav Immun 37:1-14.

Wang HM, Zhang T, Huang JK, Xiang JY, Chen JJ, Fu JL, Zhao YW (2017) Edaravone attenuates the proinflammatory response in amyloid-β-treated microglia by inhibiting NLRP3 inflammasome-mediated IL-1β secretion. Cell Physiol Biochem 43:1113-1125.

Xian H, Liou YC (2019) Loss of MIEF1/MiD51 confers susceptibility to BAX-mediated cell death and PINK1-PRKN-dependent mitophagy. Autophagy 15:2107-2125.

Xiao L, Xu X, Zhang F, Wang M, Xu Y, Tang D, Wang J, Qin Y, Liu Y, Tang C, He L, Greka A, Zhou Z, Liu F, Dong Z, Sun L (2017) The mitochondria-targeted antioxidant MitoQ ameliorated tubular injury mediated by mitophagy in diabetic kidney disease via Nrf2/PINK1. Redox Biol 11:297-311.

Xu J, Hu C, Chen S, Shen H, Jiang Q, Huang P, Zhao W (2017) Neuregulin-1 protects mouse cerebellum against oxidative stress and neuroinflammation. Brain Res 1670:32-43.

Yan H, Xiao F, Zou J, Qiu C, Sun W, Gu M, Zhang L (2018) NR4A1-induced increase in the sensitivity of a human gastric cancer line to TNFα-mediated apoptosis is associated with the inhibition of JNK/Parkin-dependent mitophagy. Int J Oncol 52:367-378.

Yu Q, Zeng KW, Ma XL, Jiang Y, Tu PF, Wang XM (2017) Ginsenoside Rk1 suppresses pro-inflammatory responses in lipopolysaccharide-stimulated RAW264.7 cells by inhibiting the Jak2/Stat3 pathway. Chin J Nat Med 15:751-757.

Zhang Q, Shi B, Ding J, Yan L, Thawani JP, Fu C, Chen X (2019) Polymer scaffolds facilitate spinal cord injury repair. Acta Biomater 88:57-77.

Zhou H, Hu S, Jin Q, Shi C, Zhang Y, Zhu P, Ma Q, Tian F, Chen Y (2017a) Mff-dependent mitochondrial fission contributes to the pathogenesis of cardiac microvasculature ischemia/reperfusion injury via induction of mROS-mediated cardiolipin oxidation and HK2/VDAC1 disassociation-involved mPTP opening. J Am Heart Assoc 6:e005328.

Zhou H, Zhu P, Guo J, Hu N, Wang S, Li D, Hu S, Ren J, Cao F, Chen Y (2017b) Ripk3 induces mitochondrial apoptosis via inhibition of FUNDC1 mitophagy in cardiac IR injury. Redox Biol 13:498-507.

Zhou H, Zhang Y, Hu S, Shi C, Zhu P, Ma Q, Jin Q, Cao F, Tian F, Chen Y (2017c) Melatonin protects cardiac microvasculature against ischemia/reperfusion injury via suppression of mitochondrial fission-VDAC1-HK2-mPTP-mitophagy axis. J Pineal Res 63:e12413.